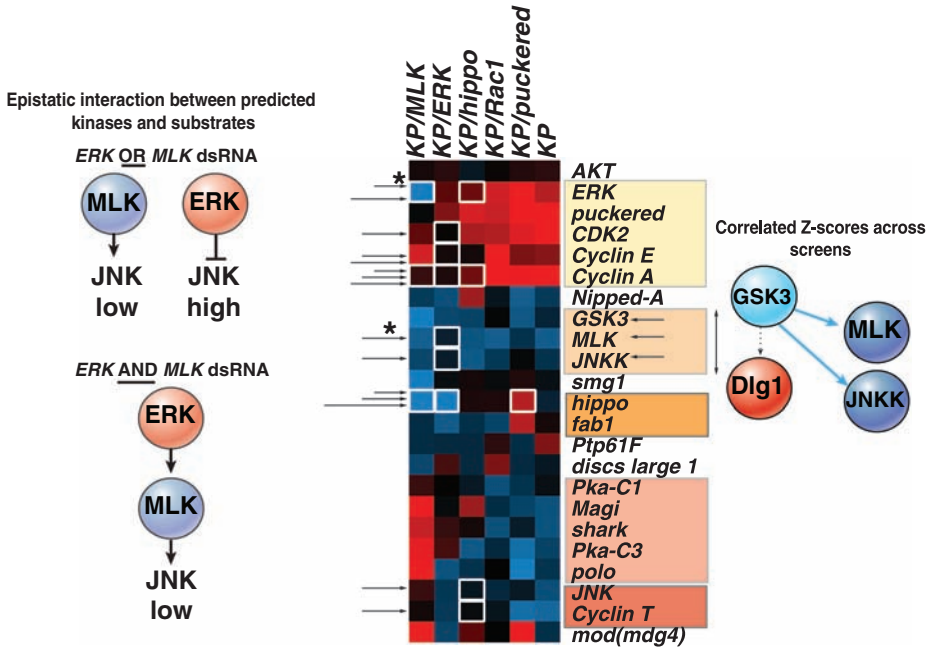

Fig. 4. Determining functional interactions among kinases and substrates in the JNK network. Hierarchical clustering of average dJUN-FRET *Z* scores after inhibition by RNAi of components in the JNK phosphorylation network in unmodified (KP), as well as in backgrounds deficient in *ERK*, *hippo*, *MLK*, or *puc*. Functional interactions are defined by the detection of an epistatic interaction between kinase and substrate (white boxes) or when the average *Z* scores of kinases and substrate dsRNAs across all sensitized screens cluster together with a cluster distance metric (an average of uncentered Pearson correlation coefficients) greater than 0.67 (shaded boxes). For example, whereas typically ERK acts as a JNK suppressor, *ERK* RNAi in *MLK*-deficient background (asterisk) leads to a notable decrease in dJUN-FRET reporter activity, which suggests that the ERK can act upstream of JNK via predicted phosphorylation of MLK and JNKK. Alternatively, GSK3 is predicted to target MLK, JNKK, and Dlg1, but only *Z* scores for GSK3, MLK, or JNKK dsRNAs cluster across screens, which suggests that GSK3-mediated phosphorylation of MLK and JNKK, but not Dlg1, is functionally relevant to JNK signaling.

24. L. J. Saucedo, B. A. Edgar, *Nat. Rev. Mol. Cell Biol.* **8**, 613 (2007).
25. P. Massimi, D. Gardiol, S. Roberts, L. Banks, *Exp. Cell Res.* **290**, 265 (2003).
26. A. Friedman, N. Perrimon, *Nature* **444**, 230 (2006).

27. We are deeply indebted to the *Drosophila* RNAi Screening Center and to J. Aach, S. Lee, C. Jørgensen, B. Mathey-Prevot, and B. Bodenmiller. The NetworKIN and NetPhorest algorithms are available at http://networkin.info and http://NetPhorest.info, respectively. This work is supported by Genome Canada through the Ontario Genomics Institute, the Spanish Ministerio de Ciencía e Innovación (BFU/Consolider 2007), and the European Union (FP6). C.B. is a Fellow of the Leukemia and Lymphoma Society. N.P. is an Investigator of the Howard Hughes Medical Institute.

Supporting Online Material
www.sciencemag.org/cgi/content/full/322/5900/453/DC1
Materials and Methods
SOM Text
Figs. S1 and S2

7 April 2008; accepted 20 August 2008
10.1126/science.1158739

Higher-Order Cellular Information Processing with Synthetic RNA Devices

Maung Nyan Win and Christina D. Smolke*

The engineering of biological systems is anticipated to provide effective solutions to challenges that include energy and food production, environmental quality, and health and medicine. Our ability to transmit information to and from living systems, and to process and act on information inside cells, is critical to advancing the scale and complexity at which we can engineer, manipulate, and probe biological systems. We developed a general approach for assembling RNA devices that can execute higher-order cellular information processing operations from standard components. The engineered devices can function as logic gates (AND, NOR, NAND, or OR gates) and signal filters, and exhibit cooperativity. RNA devices process and transmit molecular inputs to targeted protein outputs, linking computation to gene expression and thus the potential to control cellular function.

Genetically encoded technologies that perform information processing, communication, and control operations are needed to produce new cellular functions from the diverse molecular information encoded in the various properties of small molecules, proteins, and RNA present within biological systems. For example, genetic logic gates that process and translate multiple molecular inputs into prescribed amounts of signaling through new molecular outputs would enable the integration of diverse environmental and intracellular signals to a smaller number of phenotypic responses. Basic operations such as signal filtering, amplification, and restoration would also enable expanded manipulation of molecular information through cellular networks.

Molecular information processing systems have been constructed that perform computation with biological substrates. For example, protein-based systems can perform logic operations to convert molecular inputs to regulated transcriptional events (*1*–*4*). Information processing systems that perform computation on small-molecule and nucleic acid inputs can be constructed from nucleic acid components (*5*–*11*). RNA-based systems can process single inputs to regulated gene expression events (*12*, *13*) and integrate multiple regulatory RNAs for combinatorial gene regulation (*14*, *15*). We sought to combine the rich capability of nucleic acids for performing information processing, transduction, and control operations with the design advantages expected from the relative ease by which RNA structures can be modeled and designed (*16*, *17*).

We proposed a framework for the construction of single input–single output RNA devices (*18*) based on the assembly of three functional components: a sensor component, made of an RNA aptamer (*19*); an actuator component, made of a hammerhead ribozyme (*20*); and a transmitter component, made of a sequence that couples the sensor and actuator components. The resulting devices distribute between two primary conformations: one in which the input cannot bind the sensor, and the other in which the input can bind the sensor as a result of competitive hybridization events within the transmitter component. Input binding shifts the distribution to favor the input-bound conformation as a function of increasing input concentration and is translated to a change in the activity of the actuator, where a "ribozyme-active" state results in self-cleavage of the ribozyme (*21*).

Division of Chemistry and Chemical Engineering, California Institute of Technology, 1200 East California Boulevard, MC 210-41, Pasadena, CA 91125, USA.

*To whom correspondence should be addressed. E-mail: smolke@cheme.caltech.edu

The RNA device is coupled to the 3′ untranslated region (UTR) of the target gene, where ribozyme self-cleavage inactivates the transcript and thereby lowers gene expression independent of cell-specific machinery. We made simple RNA devices that function as single-input Buffer and Inverter gates that convert a molecular input to increased and decreased gene expression output, respectively (*18*).

The utility of a proposed composition framework depends partly on the extensibility of the framework itself. A framework that provides a general approach for the forward engineering of multi-input devices will allow the combinatorial assembly of many information processing, transduction, and control devices from a smaller number of components. Thus, we used defined points of integration to facilitate the assembly of putatively modular RNA components into sophisticated information processing devices (Fig. 1A) and specified three signal integration (SI) schemes (Fig. 1B). SI 1 was used to construct RNA devices that acted as logic gates (AND or NOR gates) and signal and bandpass filters through the assembly of independent single-input gates. SI 2 was used to construct devices that allowed other logic operations (NAND or OR gates) through the assembly of sensor-transmitter components linked to both stems of the ribozyme. SI 3 was used to construct devices that acted as logic gates (AND or OR gates) and exhibited cooperativity through the assembly of two sensor-transmitter components linked to a single ribozyme stem. The various operations were achieved by altering the function or input responsiveness of the single-input gates in SI 1 or sensor-transmitter components in SI 2 and 3. We assembled multiple RNA devices from various components for all operations to demonstrate the generality of the integration schemes.

In SI 1, the single-input gates act independently such that computation is performed through integration of individual gate operations in the 3′ UTR of the target transcript. Because only one of the ribozymes needs to be in an active state to inactivate the transcript, the device output (gene expression activity) is high only when both ribozymes of the single-input gates are in their inactive states. We engineered signal filters by coupling representative Buffer or Inverter gates (*18*) responsive to either theophylline or tetracycline (SI 1.1; Fig. 2A). Coupled-gate devices exhibited a device response that was shifted lower compared to that of the single-input gate, indicating the independent action of each single-input gate (Fig. 2B, SOM text S1 and S2, and table S1).

We constructed an AND gate that exhibited high output only when both inputs were present by coupling a theophylline-responsive Buffer gate and a tetracycline-responsive Buffer gate (SI 1.2; Fig. 2C). In this composition, only in the presence of both molecular inputs (theophylline and tetracycline) did both Buffer gates favor the ribozyme-inactive state, resulting in high device output (Fig. 2D and fig. S1).

We constructed a NOR gate that exhibited high output only when both inputs were absent by coupling a theophylline-responsive Inverter gate and a tetracycline-responsive Inverter gate (SI 1.3; Fig. 2E and fig. S2). In this composition, only in the absence of both inputs did both Inverter gates favor the ribozyme-inactive state, resulting in high device output (Fig. 2F and fig. S3). We also engineered a bandpass filter that exhibited high output only over intermediate input concentrations by coupling theophylline-responsive Buffer and Inverter gates (fig. S4). The various devices demonstrated that diverse information processing operations can be assembled through SI 1, where layering strategies can extend the attainable operations (SOM text S3).

Devices constructed through SI 2 and 3 consisted of multiple sensor-transmitter components, or internal gates (Fig. 1B). An internal Inverter or Buffer gate is defined as a sensor-transmitter component that activates or inactivates, respectively, a coupled component, such as an actuator or other internal gate, in the presence of input. In SI 2, the internal gates act independently through the linked ribozyme stems and therefore computation is performed through the integration of individual internal gate operations in the ribozyme core. The single ribozyme is only in the active state, corresponding to low device output, when both sensor-transmitter components are in states that activate the coupled ribozyme. We constructed a NAND gate by coupling a theophylline-responsive internal Inverter gate through stem I and a tetracycline-responsive internal Inverter gate (fig. S2) through stem II (SI 2.1; Fig. 3A). The device exhibited low output only in the presence of both inputs, because both internal Inverter gates favored the ribozyme-active state (Fig. 3B and fig. S5). Other logic operations can be performed by SI 2 devices, such as an OR operation, through the coupling of two internal Buffer gates (SOM text S4).

In SI 3, the sensor-transmitter components are coupled within a ribozyme stem, and computation occurs via the integrated operations of the internal gates. Internal gates were linked through the aptamer loop of the lower gate, IG(n), and the transmitter of the higher gate, IG(n + 1). The operation of the higher internal gate determines the state of the lower internal gate, where an internal gate can perform its encoded operation when it is in an active state, and the state of the internal gate linked to the ribozyme (IG1) determines the state of the device. We constructed an alternative AND gate by coupling a theophylline-responsive internal Buffer gate (IG1) and a tetracycline-responsive internal Inverter gate (IG2) at stem II (SI 3.1; Fig. 4A). In this composition, only in the presence of both inputs did

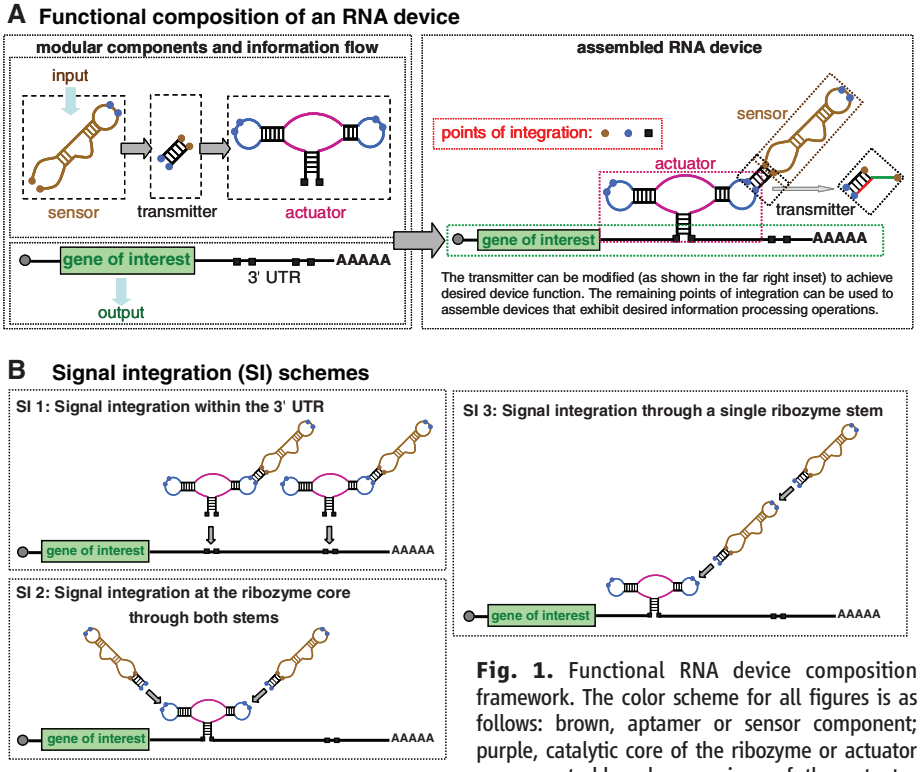

Fig. 1. Functional RNA device composition framework. The color scheme for all figures is as follows: brown, aptamer or sensor component; purple, catalytic core of the ribozyme or actuator component; blue, loop regions of the actuator component; green and red, strands within the transmitter component that participate in the competitive hybridization event. (**A**) A functional composition framework for assembling RNA devices from modular components. Information in the form of a molecular input is received by the sensor and transmitted by the transmitter to a regulated activity of the actuator, which in turn controls the translation of a target transcript as an output. (**B**) Three signal integration schemes represent different component assembly strategies to build higher-order RNA devices. The RNA device in SI 1 involves multiple actuator components controlled by single sensor-transmitter components, whereas those in SI 2 and 3 involve multiple sensor-transmitter components controlling a single actuator component.

IG1 change the state of the RNA device to favor the ribozyme-inactive state, resulting in high device output (Fig. 4B and fig. S6). We also constructed RNA devices that perform an OR operation through SI 3 (SOM text S4).

We engineered RNA devices that exhibited programmed cooperativity through SI 3 by manipulating the relative energies required to switch the device between different states (SOM text S5). RNA devices were composed of theophylline-responsive internal Buffer (IG1) and Inverter (IG2) gates (SI 3.2; Fig. 4C), in which the energetic differences between the input-unbound (**1**) and single-input–bound (**2**) states were varied (programmed through IG2; $\Delta\Delta G_{IG2}$; table S2) and the

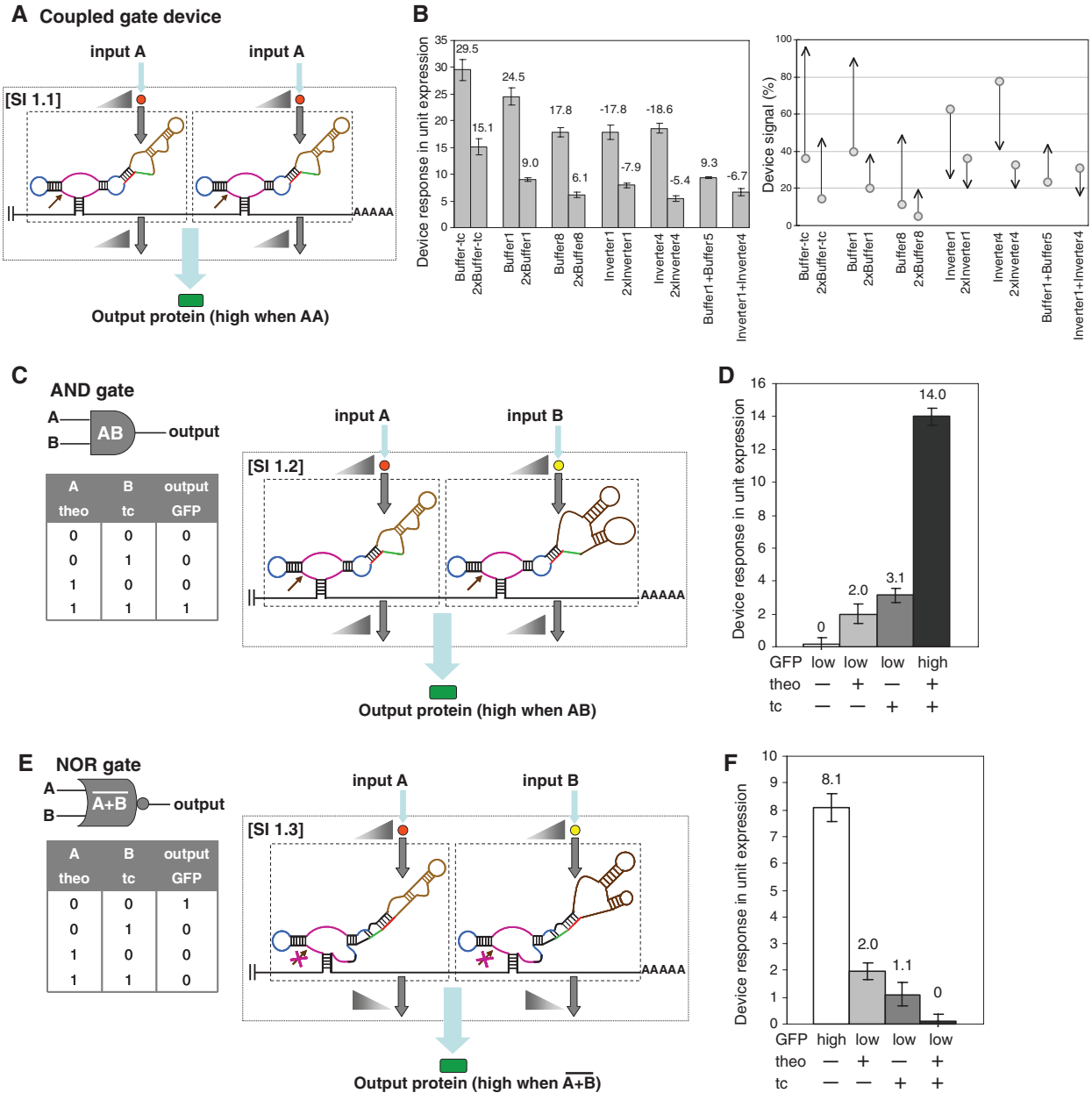

Fig. 2. RNA devices based on signal integration within the 3′ UTR (SI 1). Single-input gates are indicated in dashed boxes, and triangles indicate relationships between associated gate inputs and outputs. (**A**) An RNA device composed of two Buffer gates responsive to the same input functions to shift the device response lower than that of the single-input gate. (**B**) The device output of RNA devices composed of two single-input gates and their single-input gate counterparts. (Left) Device response (bars) is reported as the difference between gene expression activities in the absence and presence of the appropriate inputs [10 mM theophylline (theo) or 1 mM tetracycline (tc)] (*21*). (Right) Device signal (arrows) is reported over the full transcriptional range of the promoter system used as a percentage of the expression activity relative to that of an inactive ribozyme control, where circles and arrowheads indicate device signals in the absence and presence of input, respectively. The negative sign indicates the down-regulation of target gene expression by the Inverter gates. (**C**) An RNA device that performs an AND operation by coupling two Buffer gates responsive to different inputs and the associated truth table. (**D**) The device response of an AND gate (L2bulge1 + L2bulge1tc). Device response under different input conditions [theo or tc (–), 0 mM; theo (+), 5 mM; tc (+), 0.25 mM] is reported as the difference between expression activity in the absence of both inputs and that at the indicated input conditions. (**E**) An RNA device that performs a NOR operation by coupling two Inverter gates responsive to different inputs and the associated truth table. (**F**) The device response of a NOR gate (L2bulgeOff1 + L2bulgeOff1tc). Device response under different input conditions [theo or tc (–), 0 mM; theo (+), 10 mM; tc (+), 0.5 mM] is reported as the difference between expression activity in the presence of both inputs and that at the indicated input conditions. Error bars represent the SD from at least three independent experiments.

differences between the single-input–bound and two-input–bound (**3**) states were kept constant (programmed through IG1; $\Delta\Delta G_{IG1}$ = 1 kcal/mol). The devices exhibited Buffer operations and substantial degrees of cooperativity (Fig. 4D and fig. S7), where one device exhibited a degree of cooperativity [Hill coefficient (n_H) ≈ 1.65; Fig. 4E] similar to that of a naturally occurring cooperative riboswitch (*22*). We also placed internal Inverter gates into IG1 to construct a device that performed an Inverter operation and exhibited cooperativity (figs. S8 and S9). Control studies indicated that the value of $\Delta\Delta G_{IG1}$ was important to the observed cooperative response (figs. S10 and S11) and verified that the response was achieved through input binding to both sensors (figs. S12 to S15).

We have developed a composition framework for constructing higher-order RNA devices. Functional modularity is a critical element of any composition framework and was achieved in this study partly through the separation of device functions into distinct components. Although the functions of sensing and actuation frequently rely on tertiary interactions, which are not accounted for in this framework, the integration of these functions into a device is simplified via a transmitter that insulates component functions and controls the interactions between components through predictive hybridization interactions. The variety of information processing operations demonstrated from a small number of standard components emphasizes the utility of modular assembly. In addition, three of the devices have naturally occurring functional counterparts (*22*–*24*), supporting the biological

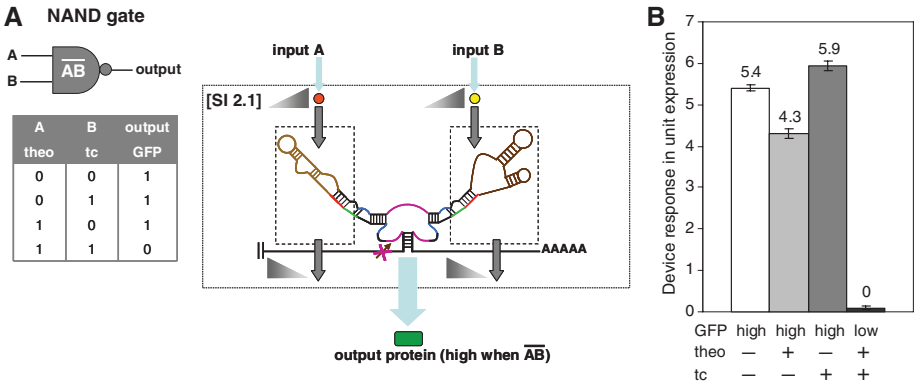

Fig. 3. RNA devices based on signal integration at the ribozyme core (SI 2). Internal gates are indicated in dashed boxes, and triangles indicate relationships between associated internal gate inputs and outputs. (**A**) An RNA device that performs a NAND operation by coupling two internal Inverter gates responsive to different inputs to different ribozyme stems and the associated truth table. (**B**) The device response of a NAND gate (L1cm10 – L2bulgeOff3tc). Device response under different input conditions [theo or tc (–), 0 mM; theo (+), 10 mM; tc (+), 1 mM] is reported as in Fig. 2F. Error bars represent the SD from at least three independent experiments.

Fig. 4. RNA devices based on signal integration at a single ribozyme stem (SI 3). Internal gates (IG*n*) are indicated in dashed boxes, and triangles indicate relationships between associated internal gate inputs and the device output. (**A**) An RNA device that performs an AND operation by coupling internal Buffer (IG1) and Inverter (IG2) gates responsive to different inputs to a single ribozyme stem. (**B**) The device response of an AND gate (tc-theo-On1). Device response under different input conditions [theo or tc (–), 0 mM; theo (+), 2.5 mM; tc (+), 0.5 mM] is reported as in Fig. 2D. (**C**) An RNA device composed of internal Buffer (IG1) and Inverter (IG2) gates responsive to the same input coupled to a single ribozyme stem. (**D**) The device response of RNA devices composed of internal Buffer and Inverter gates and their single-internal gate device counterpart (L2bulge1). Device response is reported as in Fig. 2B. Theo-theo-On10, -On11, -On12, and -On13 exhibit varying degrees of cooperativity, as quantified by Hill coefficients (n_H) greater than 1 (*26*). (**E**) The device output response of theo-theo-On13 shows a high degree of programmed cooperativity. The device response is normalized to the response at 10 mM theophylline (*21*). Error bars represent the SD from at least three independent experiments.

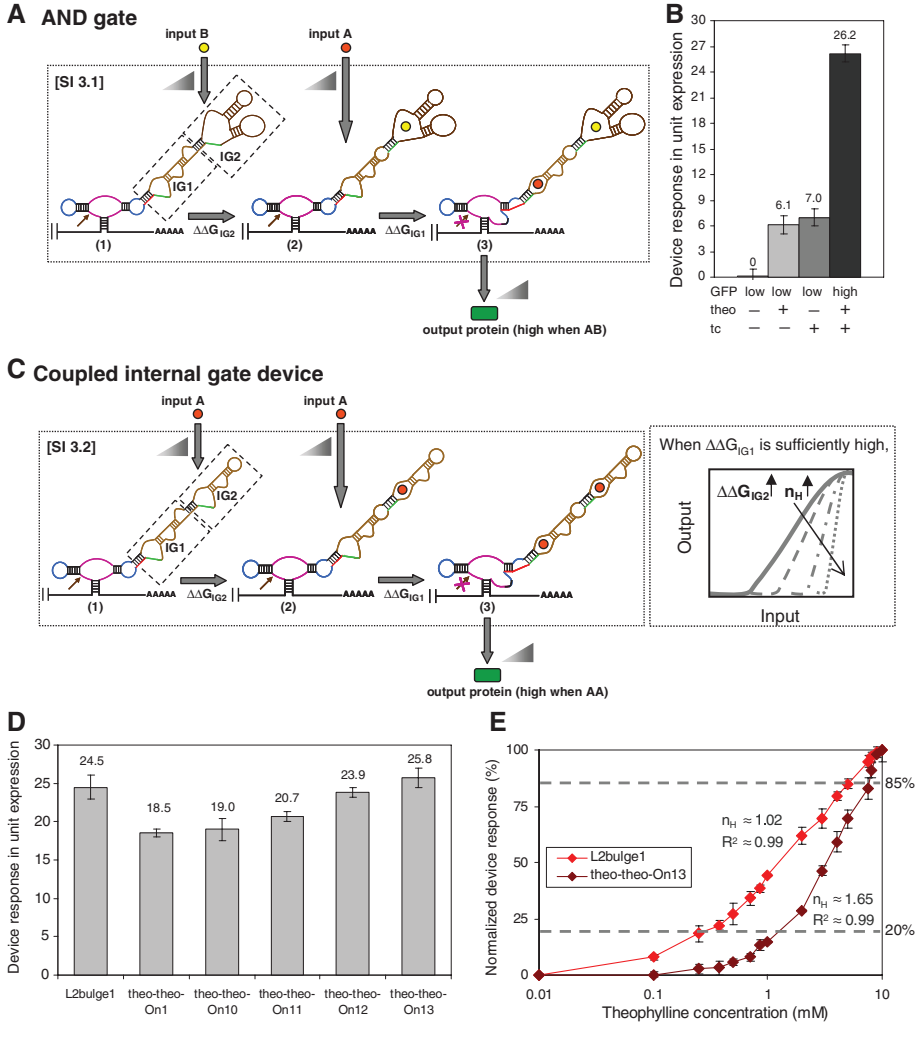

relevance of such information processing operations. The framework may be further extended to more complex devices by combining multiple SI schemes within a device and implementing layering strategies. We anticipate that further insight into RNA structure-function relationships (*25*), and improved predictions of RNA secondary and tertiary structures (*16*), may allow the development of improved modular assembly schemes, in which an important design challenge will be to insulate device functions across distinct components and control interactions between these components.

References and Notes

1. C. C. Guet, M. B. Elowitz, W. Hsing, S. Leibler, *Science* **296**, 1466 (2002).
2. B. P. Kramer, C. Fischer, M. Fussenegger, *Biotechnol. Bioeng.* **87**, 478 (2004).
3. R. S. Cox III, M. G. Surette, M. B. Elowitz, *Mol. Syst. Biol.* **3**, 145 (2007).
4. J. C. Anderson, C. A. Voigt, A. P. Arkin, *Mol. Syst. Biol.* **3**, 133 (2007).
5. G. Seelig, D. Soloveichik, D. Y. Zhang, E. Winfree, *Science* **314**, 1585 (2006).
6. Y. Benenson, B. Gil, U. Ben-Dor, R. Adar, E. Shapiro, *Nature* **429**, 423 (2004).
7. R. M. Dirks, N. A. Pierce, *Proc. Natl. Acad. Sci. U.S.A.* **101**, 15275 (2004).
8. M. N. Stojanovic, D. Stefanovic, *Nat. Biotechnol.* **21**, 1069 (2003).
9. R. Penchovsky, R. R. Breaker, *Nat. Biotechnol.* **23**, 1424 (2005).
10. R. R. Breaker, *Curr. Opin. Biotechnol.* **13**, 31 (2002).
11. M. P. Robertson, A. D. Ellington, *Nat. Biotechnol.* **17**, 62 (1999).
12. F. J. Isaacs, D. J. Dwyer, J. J. Collins, *Nat. Biotechnol.* **24**, 545 (2006).
13. B. Suess, J. E. Weigand, *RNA Biol.* **5**, 24 (2008).
14. K. Rinaudo *et al.*, *Nat. Biotechnol.* **25**, 795 (2007).
15. B. D. Brown *et al.*, *Nat. Biotechnol.* **25**, 1457 (2007).
16. M. Parisien, F. Major, *Nature* **452**, 51 (2008).
17. D. H. Mathews, D. H. Turner, *Curr. Opin. Struct. Biol.* **16**, 270 (2006).
18. M. N. Win, C. D. Smolke, *Proc. Natl. Acad. Sci. U.S.A.* **104**, 14283 (2007).
19. T. Hermann, D. J. Patel, *Science* **287**, 820 (2000).
20. A. Khvorova, A. Lescoute, E. Westhof, S. D. Jayasena, *Nat. Struct. Biol.* **10**, 708 (2003).
21. Materials and methods are available as supporting material on *Science* Online.
22. M. Mandal *et al.*, *Science* **306**, 275 (2004).
23. N. Sudarsan *et al.*, *Science* **314**, 300 (2006).
24. R. Welz, R. R. Breaker, *RNA* **13**, 573 (2007).
25. M. T. Woodside *et al.*, *Proc. Natl. Acad. Sci. U.S.A.* **103**, 6190 (2006).
26. D. L. Nelson, M. M. Cox, in *Lehninger Principles of Biochemistry* (Freeman, New York, ed. 4, 2005), pp. 167–174.

27. We thank Y. Chen, J. Liang, and D. Endy for critical reading of the manuscript and A. Babiskin for pRzS. This work was supported by the Center for Biological Circuit Design at the California Institute of Technology, the Arnold and Mabel Beckman Foundation, and the NIH. The authors declare competing financial interests in the form of a pending patent application.

Supporting Online Material

www.sciencemag.org/cgi/content/full/322/5900/456/DC1
Materials and Methods
SOM Text S1 to S6
Figs. S1 to S17
Tables S1 and S2
References

12 May 2008; accepted 12 August 2008
10.1126/science.1160311

Innate Immunity in *Caenorhabditis elegans* Is Regulated by Neurons Expressing NPR-1/GPCR

Katie L. Styer,[1] Varsha Singh,[1] Evan Macosko,[2] Sarah E. Steele,[1] Cornelia I. Bargmann,[2] Alejandro Aballay[1]*

A large body of evidence indicates that metazoan innate immunity is regulated by the nervous system, but the mechanisms involved in the process and the biological importance of such control remain unclear. We show that a neural circuit involving *npr-1*, which encodes a G protein–coupled receptor (GPCR) related to mammalian neuropeptide Y receptors, functions to suppress innate immune responses. The immune inhibitory function requires a guanosine 3′,5′-monophosphate–gated ion channel encoded by *tax-2* and *tax-4* as well as the soluble guanylate cyclase GCY-35. Furthermore, we show that *npr-1*– and *gcy-35*–expressing sensory neurons actively suppress immune responses of nonneuronal tissues. A full-genome microarray analysis on animals with altered neural function due to mutation in *npr-1* shows an enrichment in genes that are markers of innate immune responses, including those regulated by a conserved PMK-1/p38 mitogen-activated protein kinase signaling pathway. These results present evidence that neurons directly control innate immunity in *C. elegans*, suggesting that GPCRs may participate in neural circuits that receive inputs from either pathogens or infected sites and integrate them to coordinate appropriate immune responses.

Innate immune defense comprises a variety of mechanisms used by metazoans to prevent microbial infections. Activation of the innate immune system upon pathogen recognition results in a rapid and definitive microbicidal response to invading microorganisms that is fine-tuned to prevent deleterious deficiencies or excesses in the response. The nervous system, which can respond in milliseconds to many types of nonspecific environmental stimuli, has several characteristics that make it an ideal partner with the innate immune system to regulate nonspecific host defenses (*1*–*3*). However, even though a large body of evidence indicates that metazoan innate immunity is under the control of the nervous system, the mechanisms involved in the process and the biological importance of such control remain unclear. To provide insights into the neural mechanisms that regulate innate immunity, we have taken advantage of the simple and well-studied nervous and innate immune systems of *Caenorhabditis elegans.*

The powerful genetic approaches available to *C. elegans* research have been used to address central questions concerning the functions of the nervous system (*4*). With its 302 neurons and 56 glial cells, which represent 37% of all somatic cells in a hermaphrodite, the nervous system is perhaps the most complex organ of *C. elegans*. Ablation of different neurons has demonstrated that sensory neurons regulate a variety of physiological processes, including dauer formation and adult life span (*5*–*8*). In addition, *C. elegans* neurons are known to express numerous secreted peptides of the transforming growth factor–β (TGF-β) family, the insulin family, and neuropeptide families (*6*, *9*–*13*). This myriad of secreted factors has the potential to act at a distance to modulate various physiological processes by regulating the function of neuronal and nonneuronal cells throughout the animal.

Like other free-living nematodes, *C. elegans* lives in soil environments where it is in contact with soilborne microbes, including human microbial pathogens; it has evolved physiological mechanisms to respond to different pathogens by activating the expression of innate immune response genes that are conserved across metazoans (*14*–*19*). *C. elegans* also has behavioral responses to pathogenic bacteria such as *Bacillus thuringiensis* (*20*, *21*), *Microbacterium nematophilum* (*22*), *Photorhabdus luminescens* (*23*), *Pseudomonas aeruginosa* (*24*–*26*), and *Serratia marcescens* (*24*, *27*, *28*). Animals infected with these pathogens avoid lawns of the pathogen, or migrate away from pathogen odors. It is currently unknown how the nematode can sense pathogenic bacteria, although mutants in sensory-transduction molecules such as the Gi-like protein ODR-3 and the G protein–coupled receptor kinase GRK-2 are incapable of *S. marcescens* lawn avoidance (*28*). These results suggest that G protein–coupled receptors (GPCRs) may participate in neural circuits that receive inputs from either pathogens or infected sites and integrate them to coordinate appropriate defense responses.

To study the role of GPCRs in the regulation of innate immune response, we first determined the susceptibility of 40 *C. elegans* strains carrying mutations in GPCRs to the human opportunistic pathogen *P. aeruginosa* strain PA14, a clinical isolate capable of rapidly killing *C. elegans* at 25°C

[1]Department of Molecular Genetics and Microbiology, Duke University Medical Center, Durham, NC 27710, USA. [2]Howard Hughes Medical Institute and Laboratory of Neural Circuits and Behavior, Rockefeller University, New York, NY 10021, USA.

*To whom correspondence should be addressed. E-mail: a.aballay@duke.edu